Pergamon

Solid State Communications, Vol. 92, Nos 1-2, pp. 71-81, 1994
Elsevier Science Ltd
Printed in Great Britain
0038-1098/94 $7.00+.00

0038-1098(94)00491-9

ELECTRONIC PROPERTIES OF METAL DOPED FULLERIDES

T.T.M. Palstra and R.C. Haddon

AT&T Bell Laboratories, Murray Hill, New Jersey 07974

Metal doped C_{60} compounds comprise a class of materials, which includes insulators, conductors and superconductors which exhibit record superconducting transition temperatures T_c for a molecularly based solid. The moderately high values of T_c originate from the interaction of the conduction electrons with high frequency intramolecular phonons, and from the high density of states at the Fermi level. The high density of states and narrow band width arise from the small orbital overlap between the C_{60} molecules. Hence, both electron-phonon and electron-electron interactions are expected to be important features of the of the electronic structure of metal doped fullerides. Whereas superconductivity is mediated by electron-phonon interactions in the A_3C_{60} phases, we show that electron-electron interactions determine the low temperature transport properties. We compare the electronic properties of these materials with other classes of superconductors.

Keywords : A. fullerenes, superconductors. D. electronic structure, electron - electron interactions, electron - phonon interactions

Introduction

In the three years since the discovery of the metal doped fullerides,[1] [2] [3] [4] a remarkably clear picture of the superconductivity has emerged. In fact, the superconducting A_3C_{60} compounds, with A as alkali metal, form a series of compounds in which many of the properties relevant to superconductivity can be probed, yielding a textbook picture of the superconducting state which includes the effects of electron-phonon coupling and the density of states at the Fermi level together with details of the relevant phonon modes. The transition temperatures are the highest known for conventional superconductors. While certain properties relevant to their application, such as the transition temperature, critical current density and upper critical fields, are rather modest for the A_3C_{60} compounds when compared with the high temperature superconductors, the A_3C_{60} materials seem to conform to the Bardeen-Cooper-Schriefer theory of superconductivity - or even exemplify it - whereas the origin of high temperature superconductivity remains obscure.

It is generally accepted that the superconductivity in A_3C_{60} is mediated by electron-phonon interactions.[5] [6] [7] [8] The high frequency on-ball molecular vibrations are in part the origin of the high values of T_c. These phonons can be readily probed because their molecular nature removes the dispersion usually associated with the solid state. This situation is analogous to that in the clusters of the Chevrel-phase superconductors which contain Mo-S or Mo-Se bonds and thus give rise to high energy phonons. In traditional intermetallic compounds the high frequency phonons are inaccessible in real materials because structural instabilities alleviate the hardness of the material.

The second factor leading to elevated transition temperatures is the high density of electronic states at the Fermi level, $N(E_F)$, caused by the small overlap of the wave functions on adjacent C_{60} molecules. It is possible to vary $N(E_F)$ by selecting alkali metals with different ionic radii,[9] or by applying external pressure.[10] Both approaches affect the orbital overlap between C_{60} molecules and change $N(E_F)$ such that T_c can be varied from below 5K up to 32K (Figure 1).[11] The conduction band near the Fermi energy derived from the molecular t_{1u}-levels is very narrow and is estimated to be about 0.5 eV on the basis of band structure calculations.[12] [13] [14]

Therefore electron-electron interactions are expected to be an important feature of the electronic structure of these materials.[15]

In this review we focus on electronic transport measurements on A_3C_{60}. In particular, we discuss the role of electron-phonon and electron-electron interactions and their relevance for the electronic properties. We shall argue that while electron-phonon interactions govern the pairing of the conductions electrons, it is electron-electron correlations that are responsible for the low temperature electron scattering and therefore limit the conductivity. Thus the important features of transport in A_3C_{60} - both in the normal and superconducting states - originate on the C_{60} molecule. A further important issue for the electronic properties of A_3C_{60} is the fact that the conductivity is close to the Mott limit. This makes disorder an important parameter. Finally, we will compare the A_3C_{60} compounds with other superconductors for which electronic correlations are important.

Electron-phonon interactions

Four sets of phonon modes may be distinguished in the A_xC_{60} materials.[8] For the A_3C_{60} composition every mode that is coupled to the electrons in the conduction band will contribute to the total electron-phonon coupling constant V that results in a superconducting transition temperature

$$T_c = <\omega> \exp(-1/N(E_F)V) \qquad (1)$$

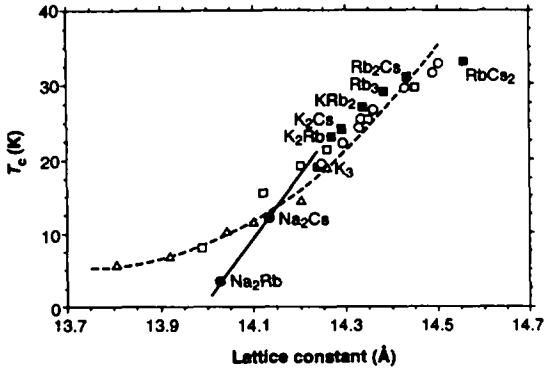

Fig.1. Superconducting transition temperature T_c versus lattice parameter for various cubic A_3C_{60} compounds. Filled and open symbols are for ambient and high pressure data, respectively. The dashed line is a LDA calculation, and the solid line is suggested for primitive cubic systems (after Prassides et al.[23])

However, the phonon modes that contribute most to the superconductivity are the high-frequency on-ball vibrations with H_g symmetry. Since these vibrations are localized on the balls, they have no dispersion and are easily observed by Raman spectroscopy.[1][16] [17] [18] [19] As may be seen in the Raman spectra shown in Figure 2, [19] alkali metal doping of C_{60} brings about large changes in the vibrational spectrum. The high frequency A_g mode serves as a reliable indicator of the number of electrons on the C_{60} molecule, and has been observed to shift to lower energy by about 6 cm^{-1} for each electron added to molecule, and this signature is often used, along with resistivity (Fig. 3)[1][20] [21] to monitor the extent of alkali metal doping. The H_g modes in particular have been implicated in the electron-phonon coupling responsible for superconductivity in A_3C_{60}. It is apparent from Figure 2 that a number of these modes are grossly modified in the A_3C_{60} phase as compared to the C_{60} and A_6C_{60} compositions. That is, they undergo shifts, broaden or disappear entirely. Many workers have concluded that the $H_g(2)$ mode assumes the largest weight in λ [$=N(E_F)V$]. Hence Raman spectroscopy and elastic neutron-scattering have become a powerful tools for the investigation of the various A_xC_{60} phases.[1][16][17][18][19][22] [23] A number of important

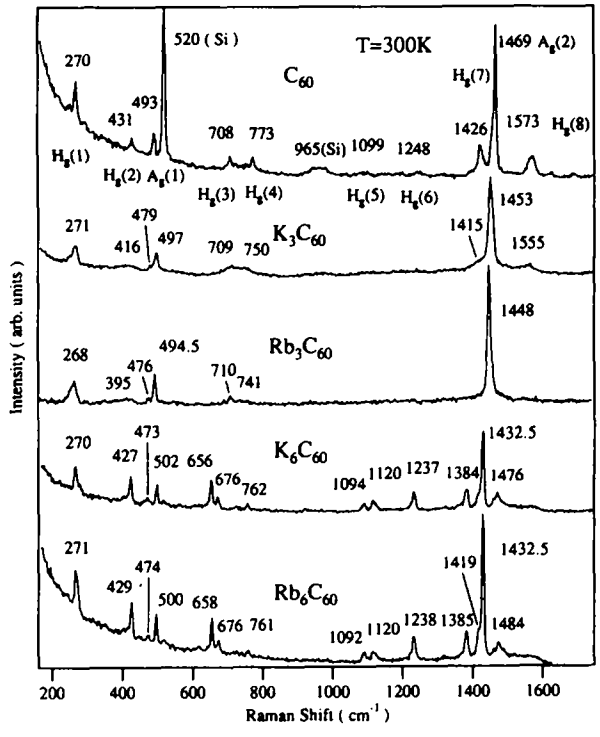

Fig.2. Raman spectra of C_{60}, K_3C_{60}, Rb_3C_{60}, K_6C_{60} and Rb_6C_{60} at T=300K (after Eklund et al.[19])

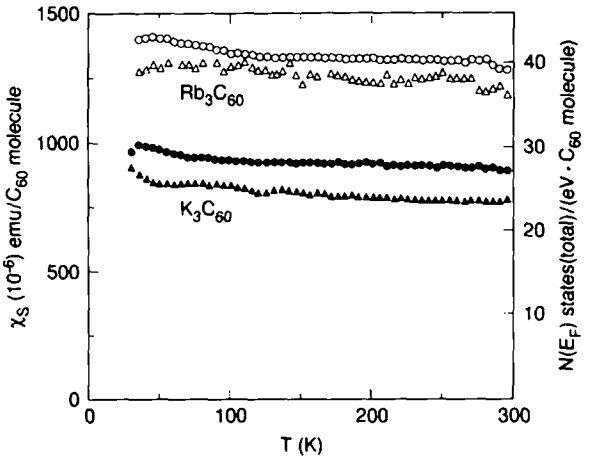

Fig.3. Composition dependence of the electrical resistivity at 333K of K_xC_{60}, Rb_xC_{60} and Cs_xC_{60}.[20]

aspects of the vibrational behavior of the A_3C_{60} materials[24] [25] [26] were anticipated by theoretical analyses, and this has lent credibility to the theoretical models and to the current level of understanding that has been attained in the field.

While metallic and superconducting phases have been observed in A_xC_{60} for A both an alkali or alkaline earth element,[27] [28] we shall discuss only the A_3C_{60} compounds where A is an alkali metal. For these compounds, charge transfer from the alkali metal to C_{60} is very close to 1 electron. For A = K and Rb the binary compounds A_3C_{60} adopt the fcc structure[29] and in these compounds superconductivity is observed at 18 and 28K, respectively. In the fcc phase there is one octahedral and two tetrahedral sites per C_{60} molecule. T_c can be raised to 33K by using ternary compounds as this approach has led to largest expansion of the fcc lattice.[30]

The transition temperature of all the binary and ternary fcc A_3C_{60} compounds depend only on the lattice parameter, in a regular manner. In general there are three parameters controlling the transition temperature: the frequency of the phonons which couple to the conduction electrons, the electron-phonon coupling strength and the density of states at the Fermi level. Since the relevant phonons are of molecular origin, their frequencies are unaffected by the dopant. Thus the only variable in these superconductors is $N(E_F)$, which is dictated by the degree of overlap of the t_{1u}-derived C_{60} molecular orbitals. Thus T_c can be continuously adjusted from T_c ~5K for Na_2RbC_{60} up to 32K for $Cs_2Rb_1C_{60}$ beyond which the cubic structure becomes unstable. Dopant variations to control the lattice parameter and thus T_c are complemented by high-pressure studies. T_c decreases under pressure at a rapid rate, approximately 1K/kbar. By taking into account the compressibility of A_3C_{60}, the T_c vs lattice parameter relationship is found to be the same for both pressure studies and alkali dopant variations. This emphasizes again the passive role played by the alkali metal counterions in the electronic properties, and supports the idea that superconductivity is determined by on-ball vibrations. The average phonon frequency extracted from eq. 1 and Fig. 2 is in the range of the C_{60} molecular vibrations, and implies a moderate electron-phonon coupling constant. For example, Extended Huckel Theory band structure calculations give $\omega \sim 700\ cm^{-1}$ and V = 0.016 eV based on the T_c values and lattice constants reported for K_3C_{60} and Rb_3C_{60}.

Superconductivity is not restricted to the fcc structure and has been shown to occur in simple cubic A_3C_{60}.[31] [32] For relatively small intercalants and lattice parameters the simple cubic structure is maintained and T_c spans the range from 3 to 10K. Interestingly, T_c shows a greater dependence on lattice parameter, implying a somewhat stronger coupling. However, the transition temperatures of the the simple cubic structures have not approached those of the fcc compounds.

Electron-electron Interactions

Because of the small overlap between the C_{60} molecules, the width of the conduction band derived from the molecular t_{1u}-levels is rather narrow. Band structure calculations indicate a value of approximately 0.5eV and as a consequence $N(E_F)$ is large. The value of $N(E_F)$ has been evaluated from a number of experiments,[15] and in Fig. 4 we show the normal state magnetic susceptibility.[25] However, due to the narrow bandwidth, electron correlations are important and this is reflected in the fact that the bare Fermi level density of states obtained from band structure calculations underestimates the values that can be derived from Fig. 3.[25][15] Various electron-electron interactions have been considered, but we attribute this behavior to a Brinkman-Rice enhancement[33] with an effective mass ratio given by $m^*/m \sim 2 - 3$. This value is similar to that observed in other organic charge transfer superconductors.[15]

Electrical Transport

Having discussed the superconducting state of the A_3C_{60} materials, we now turn to the normal state transport

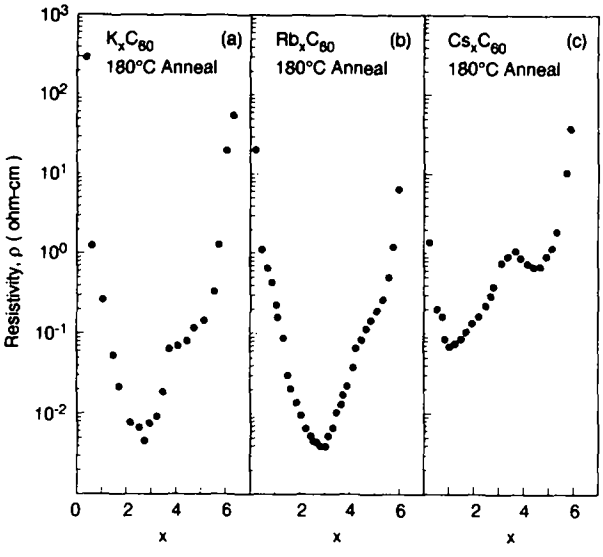

Fig.4. Temperature dependence of the static susceptibility of K_3C_{60} and Rb_3C_{60}, and density of states $N(E_F)$ (after Ramirez et al.[25])

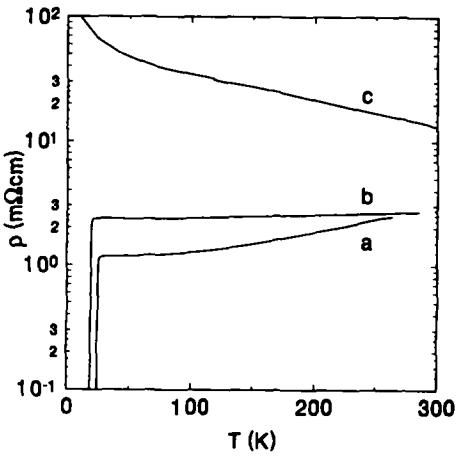

Fig.5. Temperature dependence of the electrical resistivity of underdoped (c) granular (b), and crystalline (a) thin films of K_3C_{60}.[34]

properties. As discussed above this sequence of subjects is appropriate because in contradistinction to most other compounds, the properties of the A_3C_{60} superconducting state are rather well understood. As we show below, the normal state transport properties are amenable to the same type of simple explanation which once again emphasizes the role of on-ball phenomena.

The electronic transport properties have been studied in various regimes: dc, rf, microwave and optical frequency and provide insight into various scattering processes. We expect contributions both from electron-phonon scattering (already discussed in connection with the superconductivity), as well as electron-electron scattering as a result of the narrow bandwidth. We argue that electron-electron interactions dominate at low temperature whereas electron-phonon interactions are only dominant above room temperature. Thus there are two scattering processes in the A_3C_{60} materials and each channel acts to limit the conductivity in a different temperature regime. Besides the temperature dependent scattering processes, there is a very large temperature independent contribution to the resistivity, which limits the residual resistivities to approximately 1 mΩcm.

Residual resistivity

In contrast to most metallic compounds, in which the residual resistivity ρ_o can be reduced significantly by purification and improved crystal growth, the residual resistivity of the A_3C_{60} materials is still very large and in present samples has a value of approximately 1 mΩcm. The most reliable values can be obtained in thin films, where the geometry is known within a few percent. Highly textured films exhibit ρ_o of 1.2 mΩcm for both K_3C_{60} and Rb_3C_{60} (Fig. 5).[34] Films with less texture and smaller grains exhibit larger values with ρ_o ~ 2.5 mΩcm.[35] Single crystals, in which the grain size should be large, exhibit resistivity values that are the same as those found in the crystalline films for both ρ(300K) and ρ_o.[36] The error in the determination of the absolute value of ρ_o is larger in the case of crystals due the difficulty in precisely measuring the sample geometry.

Measurements of the optical reflectivity extrapolate to a dc value for ρ_o of ~0.8 mΩcm.[37] [38] The main source of uncertainty in this experiment originates from the non-specular surface of the powder sample, and is difficult to quantify. Microwave absorption measurements were reported to yield an even smaller value, ρ_o ~ 0.6 mΩcm.[39] The most likely source of systematic error in this experiment comes from leakage of the microwave radiation through the entire thickness of the sample (millimeters), whereas it should be confined to the skin depth (~5μm).

The high frequency measurements, however, have the advantage that they probe the resistivity on a smaller length scale (microns) than the dc measurement, which probe the entire sample. If the sample exhibits a torturous current

path, (see below) the dc measurements could exhibit a systematic error and lead to an overestimate of the intrinsic resistivities. Besides the aforementioned direct determinations of ρ_o, we also discuss two powerful, but indirect measurements. First we consider the slope of the upper critical field $H'_{c2} = -dH_{c2}/dT(T = T_c)$. H'_{c2} contains both an intrinsic contribution due to the electronic parameters (clean limit), but may also contain a "dirty limit" contribution if $\ell < \xi$ (ℓ mean free path, ξ superconducting coherence length). We show later that there is strong evidence that in all samples we are in the dirty limit and thus a simple relationship obtains: $H'_{c2} \propto \gamma\rho_o$ with γ the linear electronic specific heat coefficient. γ cannot be directly evaluated from specific heat measurements at low temperature because of the superconducting gap. An estimate can be obtained, however, from the specific heat jump at T_c - for weak coupling BCS-behavior: $\Delta C = 1.43\gamma T_c$. The measurements of ΔC gives values for ρ_o that are close to the experimental values. We conclude from this that the resistivity measured on thin films is intrinsic and is not the result of a torturous current path. Moreover, this means that we can use H'_{c2} as a direct measure of the residual resistivity. The lowest H'_{c2} and thus the lowest ρ_o was reported for single crystalline K_3C_{60} with a value of 1.3 T/K.[40] The highest H'_{c2} was reported for granular thin films of K_3C_{60} with a value of 5.5 T/K. For powders H'_{c2} has been measured in a number of experiments to have the value $H'_{c2} \sim 2-4$ T/K for K_3C_{60} and Rb_3C_{60} (Fig. 6).[41] [42] [43] The variations in H'_{c2} among different sample preparations is further evidence that we are in the dirty limit.[44]

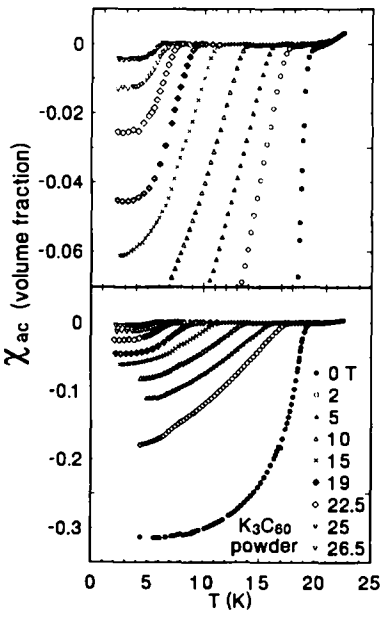

Fig.6. Temperature dependence of the ac susceptibility of K_3C_{60} powder in large magnetic fields. The upper panel shows the onset of the transition in more detail.[41]

The fluctuation conductivity above T_c provides a second indirect approach to the determination of ρ_o. In most 3d superconductors the resistivity near T_c is so small, that fluctuation effects are limited to a very narrow range of temperatures ($\Delta T/T_c \leq 10^{-6}$). However, since ρ_o is very large in A_3C_{60} it is possible to study fluctuation phenomena. For a 3d material one expects that the excess conductivity due to superconducting fluctuations will scale as $\sigma_{excess} \propto \left[(T - T_c)/T_c\right]^{-1/2}$ and this behavior was observed for single crystal K_3C_{60} (Fig. 7).[45] Usually the proportionality constant in this expression leads to the superconducting coherence length $\xi(0)$. However, the geometry is difficult to measure for doped crystals, and the authors chose to combine their results with published values of $\xi(0)$ to calculate ρ_o. They obtained a value of 0.12 mΩcm for K_3C_{60} and $\rho_o = 0.22$ mΩcm for Rb_3C_{60}, considerably smaller than the other measurements of ρ_0. It would seem desirable to repeat these experiments on well defined samples in order to obtain $\xi(0)$ directly and verify the low value of ρ_o . Measurements by the present authors on crystalline thin films did not show this scaling behavior, presumably due to the intrinsic width of the transition. In the granular films the excess conductivity obeyed a different power law $\sigma_{excess} \propto \left[(T - T_c)/T_c\right]^{-2}$, which was ascribed to zero-dimensional fluctuations (Fig. 8).[35] In simple terms, this

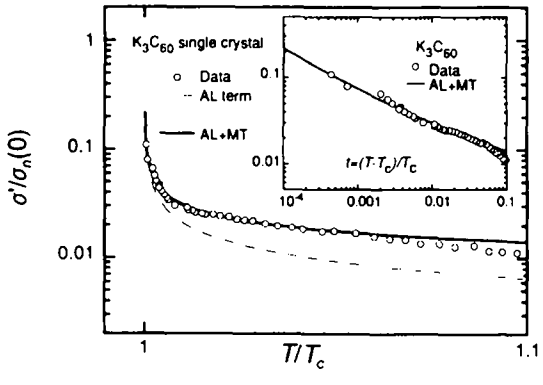

Fig.7. Normalized excess conductivity versus T/T_c for single crystal K_3C_{60}. The inset shows the normalizes excess conductivity versus reduced temperature $(T-T_c)/T_c$.[45]

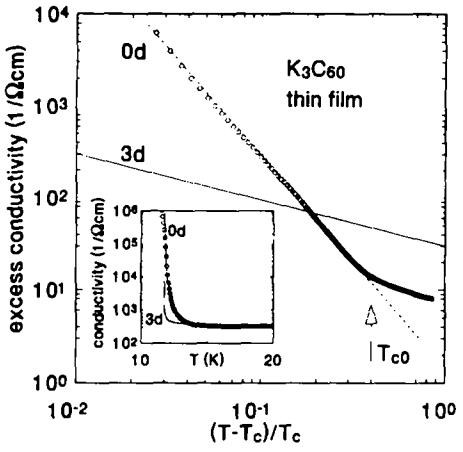

Fig.8. Excess conductivity versus reduced temperature for granular thin film K_3C_{60}. The inset compares the zero and three dimensional behavior.[35]

behavior can be observed in granular materials if the grains are weakly coupled and have a typical size smaller than the Pippard coherence length ξ_o. The grain size was estimated to be about 60Å based on X-ray diffraction measurements, whereas band structure calculations give $\xi_o \simeq 140$Å.

As we show below, the determination of ρ_o assumes considerable importance in the A_3C_{60} metals because the current data suggest a mean free path ℓ comparable to the size of a C_{60} molecule. A definitive measurement of ρ_o and ℓ could distinguish between intramolecular and intermolecular scattering processes. Various models have been suggested, including a resonant tunneling model[46] (with tunneling between adjacent C_{60} molecules), and fluctuation induced tunneling (tunneling between grains).[47] However, it must be considered surprising that these materials are metals in the first place since resistivities of 1 mΩcm are usually above the Mott limit and therefore the ground state could be a non-Fermi liquid. Therefore, we first determine the Mott limit for the A_3C_{60} materials. For a Fermi liquid description to be appropriate, we require that $k_F\ell > 1/2\pi$, with k_F the Fermi wave vector, and ℓ the mean free path at zero temperature averaged over the Fermi surface. We establish $k_F\ell$ by using the general relation between the conductivity and the Fermi surface area S_F, assuming an isotropic mean free path:

$$\sigma = \frac{e^2}{\hbar}\,\frac{1}{12\pi^3}\,(S_F\ell) \qquad (2)$$

We estimate $k_F\ell$ in two limiting cases using the free electron approximation. For a single non-interacting band with three carriers per C_{60} molecule, combined with the experimental residual resistivity of 1.2 mΩcm, eq(2) yields $k_F\ell \simeq 2.5$ as an upper bound for the mean free path at low temperatures. For the case of three degenerate parabolic bands (derived from the t_{1u} orbitals), we obtain $k_F\ell \simeq 1$. Thus the limiting conductivity $[\sigma_0 = 1(m\Omega cm)^{-1}]$ exceeds the Mott value:

$$\sigma_{Mott} = 0.01e^2k_F/\hbar \sim 0.5-0.7\ (m\Omega cm)^{-1} \qquad (3)$$

Thus a Fermi liquid description of the metallic state is appropriate. The Mott limit for A_3C_{60} is smaller than in regular metals because of the low conduction electron density. Given the validity of the Fermi liquid description for A_3C_{60}, we can obtain an estimate for ℓ. There are a number of approaches, including the use of the expression: $\ell = v_F/\tau = k_F/m^*\tau$. k_F is usually based on a single band spherical Fermi surface or Fermi surface calculations, and m^* is obtained from susceptibility measurements and the bare density of states from band structure calculations whereas τ can be estimated from high frequency conductivity experiments. We use the relation between σ and $(S_F\ell)$ given in eq (2) since it requires the fewest parameters. By using the Fermi surface area of K_3C_{60} ($S_F = 2.4 \times 10^{16}cm^{-2}$) from the band structure calculations of Erwin,[14] and our experimental value of ρ (1.2 mΩcm), we obtain $\ell = 5$Å. A similar value, $\ell = 4$Å is obtained from reflectivity data by combining the measured plasma frequency with our value for the conductivity (Fig. 9).[37] This implicitly means that the effective mass $m^* \simeq 3$, is in agreement with comparisons between theoretical and experimental determinations of the magnetic susceptibility and specific heat. In contrast with our estimate of $\ell \simeq 5$Å, there are other reports which suggest longer mean free paths. These are either based on lower ρ_o values, such as that based on the fluctuation conductivity, or higher values of the effective mass $m^* = 10$. Although the ρ_o values may yet improve with sample quality, we prefer our direct experimental value. We see no justification of $m^* \simeq 10$, since this should be observed in measurements of the magnetic susceptibility and specific heat.[25]

On-Ball Electron-Electron Scattering Model

The electrical conductivity of organic charge transfer salts[48] [49] is usually thought to be dominated by the charge transfer integral between adjacent molecules,

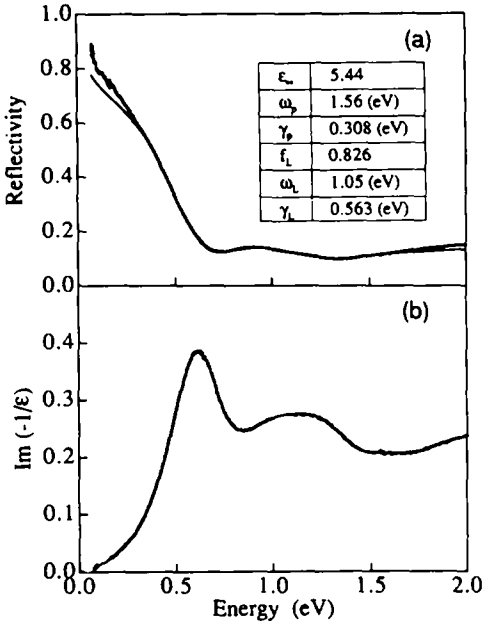

Fig.9. (a) Experimental and calculated reflectivity spectra of K_3C_{60}, shown by a thick and thin solid line , respectively. (b) Im (-1/ε) for K_3C_{60} calculated from the reflectivity spectrum by the Kramers-Kronig transformation (after Iwasa et al.[37])

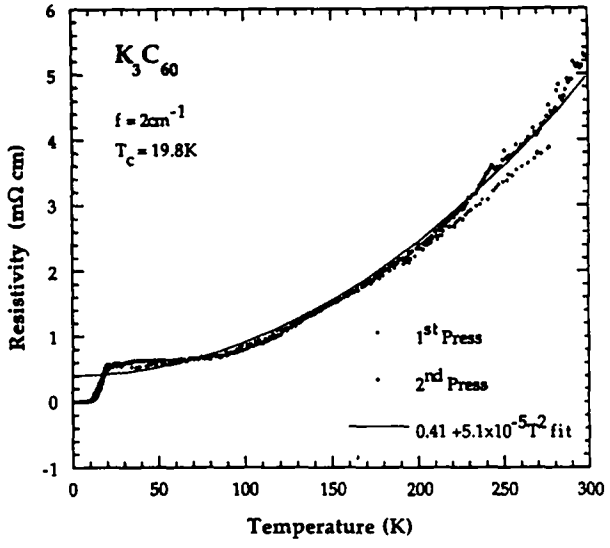

Fig.10. Temperature dependence of the electrical resistivity of K_3C_{60} evaluated from microwave surface resistivity measurements. (after Klein et al.[39])

resulting in a bandwidth that should be compared to the on-site Coulomb repulsion. However, since the mean free path $\ell \approx 5$Å is smaller than the size of a C_{60} molecule, the low temperature scattering is dominated by a process that is taking place on the C_{60} molecule. If we take the diameter of the C_{60} molecule as 7Å, then the circumference of the molecule is 22Å, and this allows conduction electrons to be placed on the molecule with a maximum separation of 7Å, in good agreement with the mean free path estimate. In this picture each electron assumes an effective "size" due to coupling with the on-ball phonon field that is responsible for the superconductivity, but it is the on-ball scattering between these quasiparticles that limits the conductivity.

Temperature dependent scattering

The low temperature resistivity has a large T^2-term, observed first in microwave reflectivity measurements (Fig. 10)[39], and later in single crystals[50] and thin films.[34] >From T_c to room temperature ρ approximately doubles from 1 to 2 mΩcm. In a three dimensional Bloch-Grüneisen model, the acoustic phonons give rise to a T^3-temperature dependence, whereas electron-electron Umklapp scattering results in a T^2 behavior. Our data on Rb_3C_{60} between 50 and 250K can be accurately fit to the expression $A * T^2 + B * T^3$ and both constants extracted to give values of $A = 10^{-2}\mu\Omega cm/K^2$ and $B = 3.6 \times 10^{-5}\mu\Omega cm/K^3$. Band structure calculations were reported to yield ρ values of 69μΩcm[51] and 160μΩcm at 260K [50][36] for the resistivity in the presence of the electron-phonon scattering. Both estimates are an order of magnitude smaller than the experimentally observed increase between T_c and 260K, suggesting that electron-phonon interactions do not determine the low temperature resistivity. A similar conclusion was drawn from high temperature resistivity measurements ($T > 300K$) where a linear temperature dependence is observed. If one interprets this behavior with electron-phonon scattering, unreasonably large values of the electron-phonon coupling constant λ are required.[46] Thus we turn to a consideration of electron-electron scattering.

The value of the electronic T^2-coefficient A can be independently estimated from:

$$A \sim \frac{1}{\omega_p^2 \tau_o} \frac{1}{T_F^2} \qquad (4)$$

with τ_o^{-1} the bare scattering rate, and ω_p the plasma frequency. ω_p depends only on the electron density and is roughly 1eV. The scattering rate can be estimated from Coulomb interactions of an electron gas with an average separation between the electrons of a_L: $\hbar/\tau_o \sim e^2/a_L = 27\,(a_o/a_L)$ eV, with a_o the Bohr

radius. This yields $\tau_o \sim 1$ eV. Using a Fermi temperature $T_F \sim 1500-2000$K, based on susceptibility measurements[25] we find that $A \sim 1 - 2^* 10^{-2} \mu\Omega$cm. Thus the magnitude of the T^2-term in the resistivity is consistent with a simple estimate based on the electronic scattering. Electron-electron scattering is important in this material because of the narrow bandwidth stemming from the small C_{60} wavefunction overlap.

However, we have argued above in support of the electron-phonon pairing mechanism for superconductivity, and usually the interactions leading to resistivity are identical to those leading to superconductivity. However, in A_3C_{60} the phonons with a large coupling to the electrons have been attributed to optical modes with energies of at least 100K. These high frequency phonons mediate superconductivity via virtual excitations, but these vibrational states will not be appreciably populated under the conditions of our experiment. Of course, the high frequency virtual phonons can induce changes in the magnitude of the T^2-resistivity by moderating the effective electron-electron interaction. Nevertheless, low temperature Raman studies show that the vibrational spectrum of A_3C_{60} superconductors does not change below T_c.[19]

Equation 4 was has been shown to be applicable to a number of materials by relating the resistivity coefficient A to γ, the linear specific heat coefficient, which is linear with T_F^{-1} (see Fig. 11).[34] [52] [53] All of the narrow band systems fall on a straight line of slope 2. The transition metals have the same slope but a different proportionality factor. For the A_3C_{60} materials we estimate γ from the specific heat jump at T_c, which results in a value of 48mJ/mole K^2.[25] This groups Rb_3C_{60} with the other narrow band systems. Of course, the origin of the narrow band is different for the various materials, arising in the present case from the small wave function overlap. Using literature values[48][49], we note that intercalated graphite is also a member of this class of materials and that KC_8 falls on this line, even though γ is an order of magnitude smaller. KC_8 is similar to A_3C_{60} in that superconductivity is mediated by high frequency optical phonons, however, it should be pointed out that in two-dimensional materials the resistivity due to acoustic phonons also gives rise to a T^2 dependence. Given the value of γ in KC_8, the resistivity can also be explained by electron-electron interactions. For the other two-dimensional organic superconductors (the ET-salts), the resistivity also exhibits T^2-temperature dependence, albeit only below ~50K. The resistivity coefficient A is far larger than expected from the Fermi temperature, and we conclude that the resistivity is dominated by acoustic phonons. There has been considerable debate about the importance of electronic correlations in the ET-based charge transfer salts.[48][49] Our phenomenological approach strongly suggests that since the electron-electron scattering makes a negligible contribution to the resistivity, the superconductivity in the conventional organic superconductors is also likely to be mediated by electron-phonon interactions. This leaves only two types of materials in which electronic correlations are thought to be involved in the superconducting state, namely the heavy fermion systems, in which the T^2-term of the resistivity dominates below a "coherence" temperature, and the high-temperature superconductors, which exhibit the well documented linear temperature dependence of the resistivity. In this connection a linear temperature dependence has been reported for K_3C_{60}.[19][54] [55]

Conclusion

In this article we have focused on the transport characteristics of the A_3C_{60} materials in the superconducting and normal states. We have adopted the

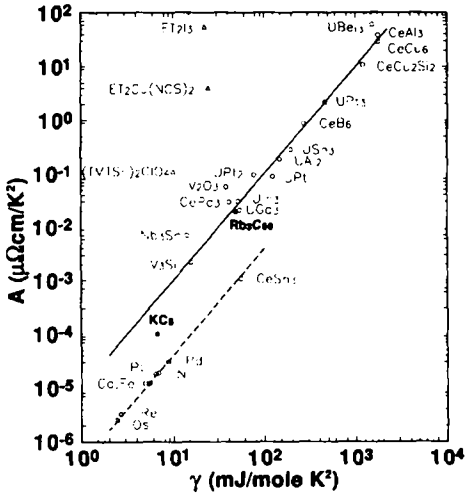

Fig.11. Resistivity coefficient A vs linear specific heat coefficient γ for wide and narrow band width conductors. The line through the heavy fermion compounds and the A15 compounds corresponds to $A/\gamma^2 = 1 \times 10^{-5}$, and includes Rb_3C_{60} and KC_8. The line through the transition metals correspond to $A/\gamma^2 = 0.4 \times 10^{-6}$. The traditional organic superconductors have much larger ratio's of A/γ^2.[34]

established view of superconductivity in these compounds which ascribes the pairing mechanism to a strong on-ball electron-phonon coupling between conduction electrons and molecular vibrations. Beyond the obvious importance of electron-phonon coupling in the superconductivity our analysis of the normal state transport has led us to conclude that the low temperature resistivity is dominated by a different interaction. Based on the temperature dependence of the resistivity and our estimate of the mean free path in A_3C_{60} at $\ell \approx 5\mathring{A}$ we ascribe the low temperature resistivity behavior to electron-electron scattering which takes place on the C_{60} molecule. Thus superconductivity and the low temperature normal state resistivity in A_3C_{60} metals are dominated by strong on-ball interactions, which are however, distinct. The band width due to overlap of the C_{60} molecules plays a similar role in both properties. Because of the narrow conduction band the Fermi temperature is low and the density of states at the Fermi level is high. The former effect enhances the role of electron-electron correlations while the latter serves to raise the T_c values to record levels for conventional superconductors.

REFERENCES

1. R. C. Haddon, A. F. Hebard, M. J. Rosseinsky, D. W. Murphy, S. J. Duclos, K. B. Lyons, B. Miller, J. M. Rosamilia, R. M. Fleming, A. R. Kortan, S. H. Glarum, A. V. Makhija, A. J. Muller, R. H. Eick, S. M. Zahurak, R. Tycko, G. Dabbagh, and F. A. Thiel, Nature **350**, 320 (1991).
2. A. F. Hebard, M. J. Rosseinsky, R. C. Haddon, D. W. Murphy, S. H. Glarum, T. T. M. Palstra, A. P. Ramirez, and A. R. Kortan, Nature **350**, 600 (1991).
3. M. J. Rosseinsky, A. P. Ramirez, S. H. Glarum, D. W. Murphy, R. C. Haddon, A. F. Hebard, T. T. M. Palstra, A. R. Kortan, S. M. Zahurak, and A. V. Makhija, Phys. Rev. Lett. **66**, 2830 (1991).
4. K. Holczer, O. Klein, S.-M. Huang, R. B. Kaner, K.-J. Fu, R. L. Whetten, F. Diederich, Science, **252**, 1154 (1991).
5. K.H. Johnson, M.E. McHenry, D.P. Clougherty, Physica C **183**, 319 (1991).
6. J.L. Martins, N. Troullier, M. Schabel, unpublished.
7. C. M. Varma, J. Zaanen, K. Raghavachari, Science **254**, 989 (1991).
8. M. Lannoo, G.A. Baraff, M. Schlüter, D. Tomanek, Phys. Rev. B **44**, 12106 (1991); M. Schlüter, M. Lannoo, M. Needels, G.A. Baraff, D. Tomanek, Phys. Rev. Lett., **68**, 526 (1992); J. Phys. Chem. Solid, **53**, 1473 (1992).
9. R.M. Fleming, A.P. Ramirez, M.J. Rosseinsky, D.W. Murphy, R.C. Haddon, S.M. Zahurak, A.V. Makhija, Nature **352**, 787 (1991).
10. O. Zhou, G.B.M. Vaughan, Q. Zhu, J.E. Fisher, P.A. Heiney, N. Coustel, J.P. McCauley, A.B. Smith, Science **255** 833 (1992).
11. K. Prassides, C. Christides, I. M. Thomas, J. Mizuki, K. Tanigaki, I. Hirosawa, and T. W. Ebbesen, Science, **261**, 950 (1994).
12. A. Oshiyama, S. Saito, N. Hamada, Y. Miyamoto, J. Phys. Chem. Solid **53**, 1457 (1992).
13. R. C. Haddon, Acc. Chem. Res., **25**, 127 (1992).
14. S. C. Erwin, in "Buckminsterfullerenes", Ed. W.E. Billups and M.A. Ciufolini, VCH New York (1993), chap 9.
15. R. C. Haddon, A. P. Ramirez, and S. H. Glarum, Adv. Mater., **6**, 316 (1994).
16. S.J. Duclos, R.C. Haddon, S.H. Glarum, A.F. Hebard, K.B. Lyons, Science **254**, 1625 (1991).
17. M.G. Mitch, S.J. Chase, J.S. Lannin, Phys. Rev. Lett. **68**, 883 (1992).
18. T. Pichler, M. Matus, J. Kurti, and H. Kuzmany, Phys. Rev. B **45**, 13841 (1992).
19. P. Zhou, K.-A. Wang, P. C. Eklund, G. Dresselhaus, and M. S. Dresselhaus Phys. Rev. B **48**, 8412 (1993).
20. R. C. Haddon, A. S. Perel, R. C. Morris, S.-H. Chang, A. T. Fiory, A. F. Hebard, T. T. M. Palstra, and G. P. Kochanski, Chem. Phys. Lett.**218** 100 (1994).
21. F. Stepniak, P. J. Benning, D. M. Poirer, and J. H. Weaver, Phys. Rev. B, 48, 1899 (1993).

22. K. Prassides, J. Tomkinson, C. Christides, M.J. Rosseinsky, D.W. Murphy, R.C. Haddon, Nature **354**, 462 (1991).

23. K. Prassides, H. W. Kroto, R. Taylor, D.R.M. Walton, W.I.F. David, J. Tomkinson, R.C. Haddon, M.J. Rosseinsky, D.W. Murphy, Carbon **30**, 1277 (1992).

24. A.P. Ramirez, A.R. Kortan, M.J. Rosseinsky, S.J. Duclos, A.M. Mujsce, R.C. Haddon, D.W. Murphy, A.V. Makhija, S.M. Zahurak, K.B. Lyons, Phys. Rev. Lett. **68**, 1058 (1992).

25. A.P. Ramirez, M.J. Rosseinsky, D.W. Murphy, R.C. Haddon, Phys. Rev. Lett. **69**, 1687 (1992).

26. C.-C. Chen and C.M. Lieber, J. Am. Chem. Soc. **114**, 3141 (1992).

27. A. R. Kortan, N. Kopylov, S. H. Glarum, E. M. Gyorgy, A. P. Ramirez, R. M. Fleming, F. A. Thiel, R. C. Haddon, Nature, **355**, 529 (1992); A. R. Kortan, N. Kopylov, S. H. Glarum, E. M. Gyorgy, A. P. Ramirez, R. M. Fleming, F. A. Thiel, and R. C. Haddon, Nature, **360**, 566 (1992).

28. R. C. Haddon, G. P. Kochanski, A. F. Hebard, A. T. Fiory, and R. C. Morris, Science, 258, 1636 (1992).

29. P. W. Stephens, L. Mihaly, P. L. Lee, R. L. Whetten, S.-M. Huang, R. Kaner, F. Diederich, K. Holczer, Nature **351**, 632 (1991).

30. K. Tanigaki, T.W. Ebbesen, S. Saito, J. Mizuki, J.S. Tsai, Y. Kubo, S. Kuroshima, Nature **352**, 222 (1991).

31. M.J. Rosseinsky, D.W. Murphy, R.M. Fleming, R. Tycko, A.P. Ramirez, T. Siegrist, G. Dabbagh, and S.E. Barret, Nature **356**, 416 (1992).

32. K. Tanigaki, I. Hirosawa, T.W. Ebbesen, J. Mizuki, Y. Shimakawa, J.S. Tsai, and S. Kuroshima, Nature **356**, 419 (1992).

33. W. F. Brinkman and T. M. Rice, Phys. Rev. B **2**, 4302 (1970).

34. T.T.M. Palstra, A.F. Hebard, R.C. Haddon, and P.B. Littlewood, accepted for Physical Review B1

35. T. T. M. Palstra, R. C. Haddon, A. F. Hebard, and J. Zaanen, Phys. Rev. Lett. **68**, 1054 (1992).

36. X.-D. Xiang, J. G. Hou, G. Briceno, W.A. Vareka, R. Mostovoy, A. Zettl, V. H. Crespi, and M. L. Cohen, Science **256** 1190 (1992).

37. Y. Iwasa, K. Tanaka, T. Yasuda, T. Koda, S. Koda, Phys. Rev. Lett. **69**, 2284 (1992)

38. L. DiGiorgy, P. Wachter, G. Grüner, S.-M. Huang, J. Wiley, and R.B. Kaner, Phys.Rev.Lett.**69** 2987 (1992)

39. O. Klein. G. Grüner, S.-M. Huang, J.B. Wiley, and R.B. Kaner, Phys.Rev.B**46** 11247 (1992).

40. J.G. Hou, V.H. Crespi, X.-D. Xiang, W.A. Vareka, G. Briceno, A. Zettl, and M. L. Cohen, Sol.St.Comm.**86**,643 (1993).

41. G.S. Boebinger, T.T.M. Palstra, A. Passner, M.J. Rosseinsky, D.W. Murphy, Phys.Rev.B**46** 5876 (1992).

42. C.E. Johnson, H.W. Jiang, K. Holczer, R.B. Kaner, R.L. Whetten, and F. Diederich, Phys.Rev.B.**46**, 5880 (1992).

43. S. Foner, E.J. McNiff,Jr, D. Heiman, S.-M Huang, and R.B. Kaner, Phys.Rev.B**46**, 14936 (1992).

44. K. Holczer, O. Klein, G. Gruner, J. D. Thompson, F. Diederich, R. L. Whetten, Phys. Rev. Lett, **67**, 271 (1991).

45. X.-D. Xiang, J. G. Hou, V. H. Crespi, A. Zettl, and M. L. Cohen, Nature 361, 54 (1993).

46. A.F. Hebard, T.T.M. Palstra, R.C. Haddon, and R.M. Fleming, Phys.Rev.B**48** 9945 (1993).

47. Z.H. Wang, K. Ichimura, M.S. Dresselhaus, G. Dresselhaus, W.-T. Lee, K.A.Wang, and P.C. Eklund, Phys.Rev.B. **48**, 10657 (1993).

48. J.M. Williams, J.R. Ferraro, R.J. Thorn, K.D. Carlson, U. Geiser, H.H. Wang, A.M. Kini, M.-H. Whangbo, "Organic Superconductors", Prentice-Hall, 1992.

49. T. Ishiguro and K. Yamaji, "Organic Superconductors", Springer-Verlag, 1990.

50. V.H. Crespi, J.G. Hou, X.-D. Xiang, M.L. Cohen and A. Zettl, Phys.Rev.B**46** 12064 (1992).

51. V. P. Antropov, O. Gunnarsson, and A. I. Liechtenstein, Phys. Rev. B, **48**, 7651 (1993).

52. K. Kadowaki and S.B. Woods, Sol.St.Comm.**58**, 507 (1972).

53. K. Miyake, T. Matsuura, and C.M. Varma, Sol.St.Comm.**71** 1149 (1989).

54. Y Maruyama, T. Inabe, H. Ogata, Y. Achiba, S. Suzuki, K. Kikuchi, I. Ikemoto, Chem. Lett, **10**, 1849 (1991).

55. W. A. Vareka, K. Khazeni, and A. Zettl, Bull.Am.Phys.Soc. **39**, 404 (1994).